batteries

MDPI

Article

Effects of Electrolyte Solvent Composition on Solid Electrolyte Interphase Properties in Lithium Metal Batteries: Focusing on Ethylene Carbonate to Ethyl Methyl Carbonate Ratios

Paul Maldonado Nogales, Sangyup Lee, Seunga Yang and Soon-Ki Jeong *

Department of Energy Engineering, Soonchunhyang University, Soonchunhyang-ro 22-gil, Sinchang-myeon, Asan-si 31538, Chungcheongnam-do, Republic of Korea; maldonado@sch.ac.kr (P.M.N.); 20237450@sch.ac.kr (S.L.); tmddk1107@sch.ac.kr (S.Y.)

* Correspondence: hamin611@sch.ac.kr; Tel.: +82-10-3131-4795

Abstract: This study investigated the influence of variations in the mixing ratio of ethylene carbonate (EC) to ethyl methyl carbonate (EMC) on the composition and effectiveness of the solid electrolyte interphase (SEI) in lithium-metal batteries. The SEI is crucial for battery performance, as it prevents continuous electrolyte decomposition and inhibits the growth of lithium dendrites, which can cause internal short circuits leading to battery failure. Although the properties of the SEI largely depend on the electrolyte solvent, the influence of the EC:EMC ratio on SEI properties has not yet been elucidated. Through electrochemical testing, ionic conductivity measurements, Fourier transform infrared spectroscopy, and X-ray photoelectron spectroscopy, the formation of Li_2CO_3, LiF, and organolithium compounds on lithium surfaces was systematically analyzed. This study demonstrated that the EC:EMC ratio significantly affected the SEI structure, primarily owing to the promotion of the formation of a denser SEI layer. Specifically, the ratios of 1:1 and 1:3 facilitated a uniform distribution and prevalence of Li_2CO_3 and LiF throughout the SEI, thereby affecting cell performance. Thus, precise control of the EC:EMC ratio is essential for enhancing the mechanical robustness and electrochemical stability of the SEI, thereby providing valuable insights into the factors that either enhance or impede effective SEI formation.

Keywords: ethylene carbonate; ethyl methyl carbonate; organolithium; SEI formation; electrolyte layer; Li electrodes

check for updates

Citation: Nogales, P.M.; Lee, S.; Yang, S.; Jeong, S.-K. Effects of Electrolyte Solvent Composition on Solid Electrolyte Interphase Properties in Lithium Metal Batteries: Focusing on Ethylene Carbonate to Ethyl Methyl Carbonate Ratios. *Batteries* **2024**, *10*, 210. https://doi.org/10.3390/batteries10060210

Academic Editor: Hirotoshi Yamada

Received: 7 May 2024
Revised: 29 May 2024
Accepted: 13 June 2024
Published: 16 June 2024

1. Introduction

In lithium-metal batteries, wherein the redox reaction of lithium ions serves as an electrode reaction, a proper understanding of the solid electrolyte interphase (SEI) layer is essential [1–4]. This layer, which is formed on the surface of the lithium anode, is crucial for battery performance because it prevents the continuous decomposition of the electrolyte solution on the thermodynamically unstable lithium anode [5,6]. In addition, understanding the SEI facilitates the suppression of the growth of dendritic lithium, which poses a significant safety risk. The properties of the SEI are heavily dependent on the composition of the electrolyte, particularly the type of solvent and lithium salt used. Typically, electrolytes are prepared by dissolving Li salts in a mixture of organic solvents. This mixture includes cyclic carbonates, such as ethylene carbonate (EC), which enhance the dissociation of lithium salts, and linear carbonates, such as ethyl methyl carbonate (EMC), which reduce viscosity and improve ionic mobility, particularly at lower temperatures [7–11].

Considering that cyclic and linear solvents fulfill distinct functions, the battery performance is likely influenced by the proportion of each solvent in the electrolyte solution. It can be assumed that this influence is closely related to the SEI because the SEI is generated through the electrochemical decomposition of the electrolyte solution [12–19]. However, studies on the effect of the solvent ratio on the properties of SEIs are scarce. Thus, this

study aimed to investigate the effects of different solvent ratios on the characteristics of SEIs in lithium metal batteries using an electrolyte solution containing EC and EMC, which are representative of cyclic and linear carbonates, respectively. Through a comprehensive examination of the interactions between these solvent mixtures and the SEI on the lithium anode, this study elucidated the mechanisms governing SEI formation and stability. The investigation focused on the influence of the variations (dependent on the solvent) on the formation of key byproducts, such as lithium oxides (Li_2O), lithium carbonates (Li_2CO_3), and organolithium compounds [20–26], which are crucial for the structure and functioning of SEI, thereby directly affecting the battery performance.

2. Materials and Methods

2.1. Electrode and Electrolyte Materials

Li metal electrodes with a thickness of 500 μm were sourced from Honjo Metal Co., Osaka, Japan, and were used as received. Anhydrous, battery-grade $LiPF_6$ (≥99.9%), EC (≥99.9%, H_2O < 5 ppm), and EMC (≥99.9%, H_2O < 5 ppm) were obtained from Enchem Co., Chungbuk, Republic of Korea. These materials were used to prepare the electrolyte solutions without further purification. To prevent moisture absorption and degradation, the chemicals were stored under an argon atmosphere in a glove box (model SK-G1200, Three-Shine Inc., Daejeon, Republic of Korea) with a dew point of −70 °C.

2.2. Electrolyte Formulations

Electrolytes with varying compositions were prepared by dissolving 1 mol dm^{-3} (M) of $LiPF_6$ in mixtures of EC and EMC at different volume ratios. The EC:EMC ratios used were 1:0, 10:1, 5:1, 3:1, 1:1, 1:3, 1:5, 1:10, and 0:1 (v/v). This arrangement encompasses a wide range of compositions, including instances where either EC or EMC is present at high concentrations, as well as several intermediate ratios. A more detailed study was conducted by observing the formation of reaction sub-products and analyzing their effects on SEI formation. These mixtures are referenced by their respective volume ratios throughout this paper for clarity and ease of reference. To minimize the moisture content, EC and EMC were dried over molecular sieves for 48 h prior to use. Subsequently, the salts and solvents were combined in a glass vial and stirred until they were fully dissolved, resulting in a clear solution. The final electrolyte preparations were confirmed to have a water content of less than 15 ppm via Karl Fischer titration.

2.3. Material Characterizations

The conductivities of the electrolytes were assessed using a conductivity meter (S230 SevenCompact, Mettler-Toledo, Switzerland) under an Ar atmosphere to avoid HF formation. The conductivity of each electrolyte was measured three times, and the average values were reported. Metallic Li disks (15.3 mm diameter) were immersed in various prepared electrolytes for 15 h at 25 °C. Following immersion, the disks were rinsed with EMC for no more than 10 min and dried under vacuum for 10 h to remove any residual EMC. Fourier transform infrared (FTIR) spectra were obtained from the surface films on the Li metal electrodes post-immersion using a Bruker FTIR spectrometer (Vertex 80V, Ettlingen, Germany) equipped with a liquid-nitrogen-cooled detector (Kolmar Technologies KMPV8-1-J2, with a 8 μm bandgap). The spectrometer was operated in vacuum to prevent the formation of HF. Consequently, the data were obtained by averaging 128 pulse sequences at each probe wavelength. The same metallic Li samples were then transferred to the X-ray photoelectron spectroscopy (XPS) load lock chamber in a sealed aluminum bag to prevent contact with atmospheric oxygen and moisture. Further, XPS analysis was conducted using an XPS instrument (K-Alpha, Thermo Fisher Scientific, Waltham, MA, USA) with an Al Kα source (E_photon = 1486.6 eV), filament current of 3 mA, and filament voltage of 12 kV. The analyzed area was 400 μm × 400 μm, with Ar etching performed every 100 s for fifteen cycles. Spectral fitting was performed using the Thermo Avantage v5.9912 software. The energy scale for the anode spectra was calibrated using the hydrocar-

bon peak (284.4 eV) as a reference. Further, the sputtering rate, calibrated separately on tantalum, was approximately 3 nm min^{-1} using 1486.6 eV Ar^+ ions.

2.4. Electrochemical Measurements

Electrochemical polarization tests were conducted using symmetrical 2032-type coin cells with Li metal serving as both the counter and working electrodes. The current density was set at 3.7 mA cm^{-2}, with a corresponding capacity of 0.6167 mAh cm^{-2} per cycle. A Celgard separator (16 μm thickness, Celgard A273, Celgard Korea, Inc., Chungbuk, Republic of Korea) was utilized. Prior to conducting the measurements, each bulk Li electrode underwent a 15 h stabilization period in the electrolyte. Electrochemical cycling tests were performed by assembling coin cells using Li metal and $LiCoO_2$ (LCO, David Technologies, Chungnam, Republic of Korea) as the counter and working electrodes, respectively. The LCO had a coating surface density of 200 g m^{-2} on a 15-μm-thick aluminum foil. Nine different electrolyte solutions, each featuring a unique EC:EMC volume ratio, were prepared with 1 M $LiPF_6$. Each cell used 100 μL of the electrolyte solution. For each electrolyte composition, cells were cycled galvanostatically at a 1 C rate (145 mA g^{-1}) between 3 and 4.15 V using a battery test system (WBCS 3000, Wonatech Co., Ltd., Seoul, Republic of Korea).

3. Results

3.1. Electrochemical Performance and Stability

Li metal foil was selected as the working electrode in this study to examine the interfacial properties between the electrode and electrolyte solution. In cells with lithium-metal electrodes immersed in an electrolyte solution for 15 h, electrochemical polarization tests revealed that the cycling voltage profile was significantly affected by the EC and EMC ratios in the solution. Figure 1a illustrates a consistent trend; decreasing the proportion of EC in the mixture substantially reduced the number of cycles. For example, the EC:EMC ratios of 1:0 and 10:1 resulted in cycling lengths of 900 and 2000 cycles, respectively. However, the number of cycles decreased drastically to approximately 10 when the EC:EMC ratio was 0:1. Further, intermediate EC:EMC ratios of 5:1 and 3:1 sustained stable voltage cycling for approximately 1200 cycles, whereas electrolyte solutions with higher EMC proportions (e.g., 1:1, 1:3, 1:5, and 1:10) yielded significantly shorter cycle lives (200–800 cycles), which were markedly lower than those with higher EC proportions. Moreover, electrolytes with very high EC proportions (e.g., 1:0 and 10:1) demonstrated highly unstable voltage behavior from the onset of the cycling process. In contrast to the other ratios, where the voltage stability may gradually deteriorate, the voltage was unstable from the outset of the cycle. Furthermore, whereas the other electrolyte solutions exhibited rapid voltage increases at specific cycles, the cell voltage increased gradually in these cases. This disparity in the electrochemical polarization behavior may be closely related to the SEIs formed on the Li metal surface, which serve as pathways for lithium ions and help stabilize the surface. As mentioned in Section 1, SEI components are generated via the electrochemical decomposition of the electrolyte solution. Thus, both the EC and EMC are crucial for the formation of an effective SEI.

The influence of the solvent ratio is further supported by the LCO discharge capacity of the Li/LCO cell. As shown in Figure 1b, a lower proportion of EC was correlated with an earlier decline in the discharge capacity. This behavior generally followed a trend consistent with the cycling behavior observed in Li/Li cells, except for the 1:0 ratio, which lacked an EMC. The reasons for the different cycling behaviors of the two types of cells (Li/Li and Li/LCO) at a 1:0 ratio remain unclear; however, variations in the electrochemical cycling conditions are suspected to have played a significant role. The required cycling time was 10 min for the former cell and 2 h for the latter. In addition, at the start of the cycle, the discharge capacity of LCO was relatively high in the electrolyte solutions with ratios of 1:1, 1:3, and 1:5. Thus, factors beyond the SEI layer, including other components

of the electrolyte solution, could influence the cell performance. To further investigate the performance discrepancies, the ionic conductivities of the electrolytes were analyzed.

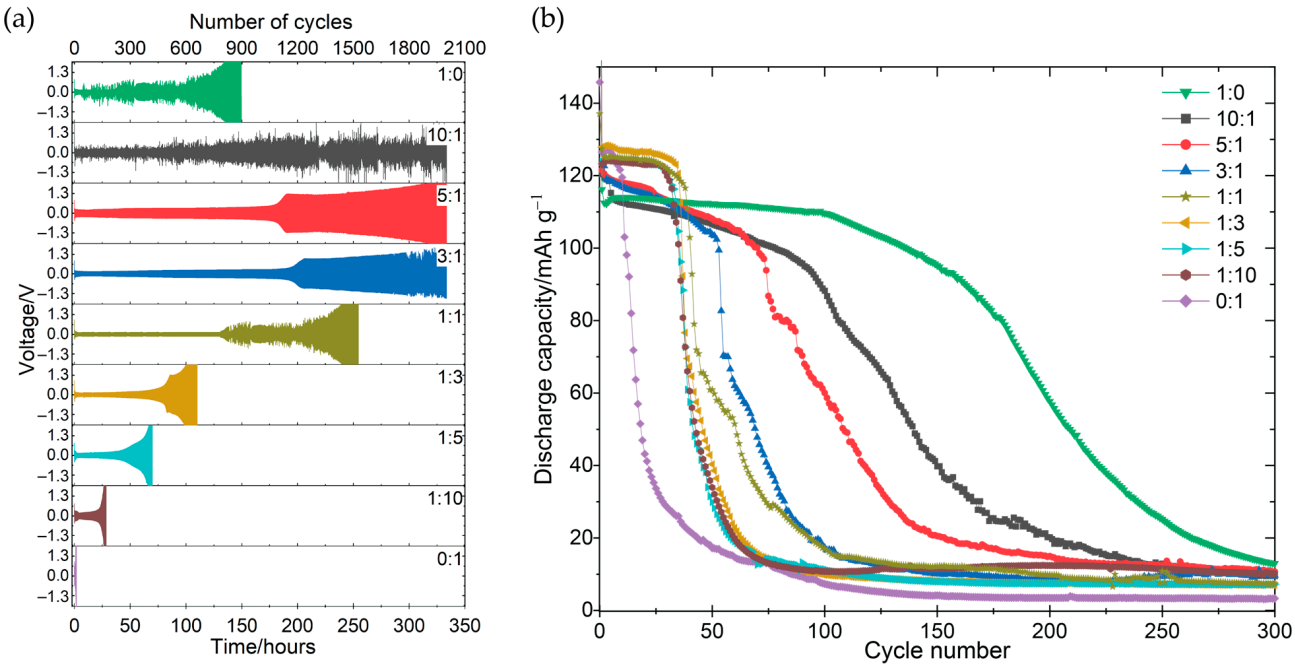

Figure 1. Electrochemical cyclability of both Li/Li and Li/LCO cells. (**a**) Voltage profile evolution during consecutive Li plating/stripping in Li/Li symmetric cells, following 15 h of immersion in a solution of 1 M $LiPF_6$ dissolved in various EC/EMC ratios, until a short-circuit occurs. (**b**) Discharge capacity of LCO as a function of cycling number in Li/LCO cells, employing the same immersion protocol and identical electrolyte mixtures.

3.2. Ionic Conductivity in EC:EMC Mixtures

A thorough examination of ionic conductivity revealed significant variations among the nine electrolyte solutions. The conductivity peaked at an EC:EMC ratio of 1:3, reaching 21.5 mS cm^{-1}. This surpassed the conductivities of both pure EC (19.54 mS cm^{-1}) and pure EMC (9.69 mS cm^{-1}). The decrease in ionic conductivity with an increase in EMC content, until pure EMC is reached, has been observed for electrolyte solutions with both high-permittivity and low-viscosity solvents [27,28]. This trend reflects the relationship between the number and mobility of ions in these solutions. This excellent ionic conductivity correlates with the observation that LCO displays the highest discharge capacity at this specific EC:EMC ratio, as mentioned in the previous section. For continuous redox reactions of lithium ions, the ions must move quickly from the bulk of the electrolyte solution to the electrode surface, or vice versa. Therefore, optimal lithium-ion mobility within the electrolyte solution is essential for fully exploiting the inherent capacity properties of the electrode material. All the ionic conductivities presented in Figure 2 suggest that a balanced mixture of EC and EMC enhanced ion transport, leveraging their complementary properties. The observed high ionic conductivity likely reflected a balance between the solvation capabilities of EC and the mobility-enhancing properties of the EMC. Maintaining an EC:EMC volume ratio between 1:5 and 1:1 is crucial. Failure to maintain this balance can result in severe electrolyte decomposition and rapid cell failure [1]. These results reaffirmed that appropriate solvent–solvent interactions stabilized the electrolyte and that the volume ratio was a critical factor for achieving a sufficiently stable SEI that supports a high discharge capacity.

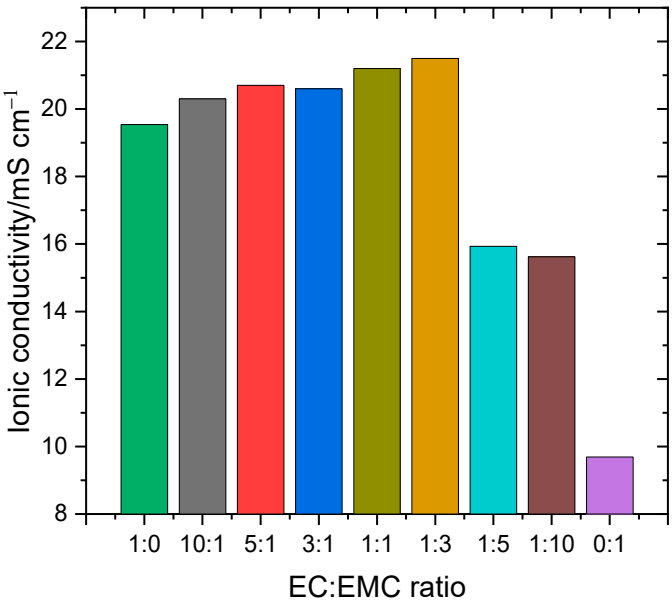

Figure 2. Ionic conductivity of electrolyte solutions prepared with various EC:EMC ratios, each containing 1 M $LiPF_6$.

3.3. Composition and Structural Analysis of SEI

Building upon previous observations, a more in-depth analysis of the products formed on the electrode surface by the decomposition of the electrolyte solution was conducted using FTIR. Figure 3 shows the FTIR spectra of the Li metal electrodes treated with nine different electrolyte solutions, illustrating the distinct electrochemical reduction products. The reduction of EC formed the dimer $(CH_2OCO_2Li)_2$, which exhibited infrared absorption peaking at approximately 1780 cm^{-1}. In contrast, the reduction of EMC yielded various alkyl carbonate compounds ($ROCO_2Li$) and alkoxide species (ROLi), with absorption peaks between 1100 and 1000 cm^{-1} [29,30]. These distinctive reduction products are evidenced by the observed variations in the FTIR peak intensities and positions, as shown in Figure 3.

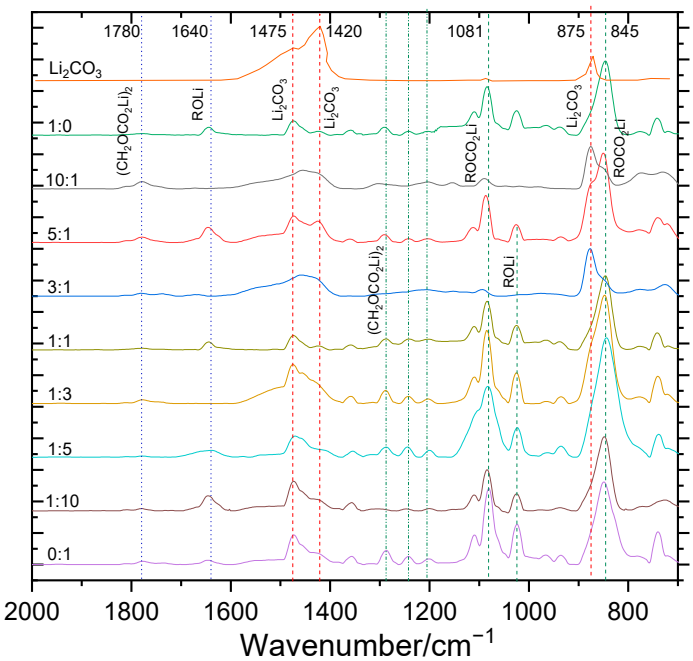

Figure 3. FTIR spectra of solid precipitates formed on Li metal electrodes from reactions between $LiPF_6$, EC, and EMC after electrolyte immersion.

After immersion in the electrolyte, the Li electrodes exhibited pronounced peaks between 1480 and 1420 cm^{-1}, characteristic of inorganic carbonates such as Li_2CO_3. The spectra of pure Li_2CO_3 are shown in Figure 3. A broad band between 1300 and 200 cm^{-1} likely indicates several absorptions, possibly attributable to the dimer $(CH_2OCO_2Li)_2$. Peaks associated with $ROCO_2Li$ species appeared at approximately 1080 cm^{-1}, and those for ROLi were visible at approximately 1025 cm^{-1}. Unfortunately, the Li_2CO_3 peaks coincided with those of other alkyl species, with pronounced peaks between 890 and 800 cm^{-1}, representing combinations of 875 cm^{-1} (Li_2CO_3) and 845 cm^{-1} ($ROCO_2Li$). Nevertheless, these spectral results indicated that the SEI films on the electrodes with ratios of 1:0, 10:1, 5:1, and 3:1 were enriched in inorganic carbonates and $ROCO_2Li$. At higher EMC ratios (1:1, 1:3, 1:5, 1:10, and 0:1), the dominant reduction products were a mixture of Li_2CO_3 and $ROCO_2Li$. These results demonstrate that the reactions of EC and EMC with $LiPF_6$ in the electrolyte solution resulted in the formation of organolithium compounds and Li_2CO_3 on the Li metal surface. Thid reflected the interaction of Li^+ with the solvent and the development of the SEI layer across all tested ratios.

The greater reactivity toward electrolyte solvent oxidation on the Li metal surface was further confirmed by XPS analysis of C 1s, as illustrated in Figures 4 and S1. Figure 4a illustrates the profile of the SEI composition across the 16 layers of the Li metal surface, where each row represents the atomic percentage of each component, detailing the transition from the outermost to the innermost layer following a multiple Ar etching processes. This heatmap-style technique quantified each component within its respective layer relative to the composition of the SEI on Li metal. Figure S1 indicates that the SEI film formed on the Li metal exhibited two pronounced peaks at 284.8 and 290 eV in the C 1s spectra, corresponding to adventitious hydrocarbon and Li_2CO_3, respectively. Three smaller peaks at 286.3 eV corresponded to organolithium compounds, including alkoxides (ROLi) and alkyl carbonates (RCH_2OCO_2Li), which contain carbon-oxygen single bonds (C-O). Moreover, the peak at 286.9 eV implied the presence of carbonyl-containing compounds (C=O), including aldehydes, $ROCO_2Li$, lithium alkyl carbonate, and carboxylic acids. This peak may also indicate the presence of acetals containing an ether-like O-C-O group. Finally, the peak at 288.7 eV indicated the presence of esters or carboxylates containing the O=C-O group. These organolithium compounds are depicted in olive-green color in Figure 4a.

The varied surface profiles illustrated that the elemental composition was predominantly Li_2CO_3, with a notably low presence of organolithium compounds despite the higher EC content. Although the organic species were evident in the FTIR analysis, they were rarely detected in the XPS results. This decrease in organolithium species implies that the predominant reaction pathways—specifically the reduction of EC to $(CH_2OCO_2Li)_2$ and ethylene (CH_2=CH_2), followed by the formation of Li_2CO_3 from intermediate species such as $LiCO_3^-$—favored the formation of Li_2CO_3 over organolithium intermediates. Even at high EC concentrations, reactions such as $LiCO_3^-(aq) + Li(EC)_4(l) \rightarrow Li_2CO_3(s) + 4EC(l)$ and $LiCO_3^- + EC(l) \rightarrow (CO_3CH_2CH_2OCO_2Li)$ predominantly facilitated the formation of inorganic compounds. The overall content of Li_2CO_3 remained below 1.5%, underscoring its significant role in the formation of inorganic components within the SEI, as illustrated in Figure S2 of O1s. The O 1s spectrum exhibited three peaks at 528.3, 531.2, and 533.9 eV, corresponding to Li_2O (light blue), Li_2CO_3 (yellow), and $ROCO_2Li$, respectively.

The formation of Li_2CO_3 observed in our experiments can be attributed to several pathways. Water is one source of Li_2CO_3 in the system, and it can enter in tiny amounts directly from any water present as a contaminant in the electrolyte [31,32]. This process resulted in the formation of Li_2CO_3 through reactions such as $CH_3OCO_2Li + H_2O \rightarrow CO_2 + CH_3OH + Li_2CO_3$. Other reactions associated with the formation of Li_2CO_3 include $2CO_2 + 2e^- + 2Li^+ \rightarrow Li_2CO_3 + CO$, $Li_2O + CO_2 \rightarrow Li_2CO_3$, and $2LiOH + CO_2 \rightarrow Li_2CO_3 + H_2O$. These pathways illustrate how lithium metal is sensitive to various environmental factors and the importance of Li_2CO_3 formation from multiple sources. Further, the higher EMC concentration in these formulations facilitates more extensive EMC reduction reactions and organolithium formation, exemplified by $CH_3CH_2OCO_2CH_3(l) + Li^+(aq) \rightarrow CH_3CH_2O(CO_2CH_3)Li(s)$

and $CH_3CH_2O(CO_2CH_3)Li(s) + Li^+(aq) \rightarrow CH_3CH_2OLi(s) + CH_3OCO_2Li(s)$. Moreover, the detection of organolithium species such as ROLi, RCH_2OCO_2Li, and $ROCO_2Li$ increased by approximately 0.25%. Furthermore, contrary to previous findings, the content of LiF species, widely known as a stabilizer of the SEI [33–35], was slightly elevated at EC:EMC ratios ranging from 1:5 to 0:1 (Figure 4b), with a Li_2CO_3:LiF ratio of approximately 1:7. In contrast, in samples with ratios of 1:1 and 1:3, this ratio was approximately 1:4. An unexpected observation was that an excess of LiF, rather than enhanced stability, facilitated the formation of a thicker SEI layer, primarily composed of LiF and Li_2CO_3, compared to other samples.

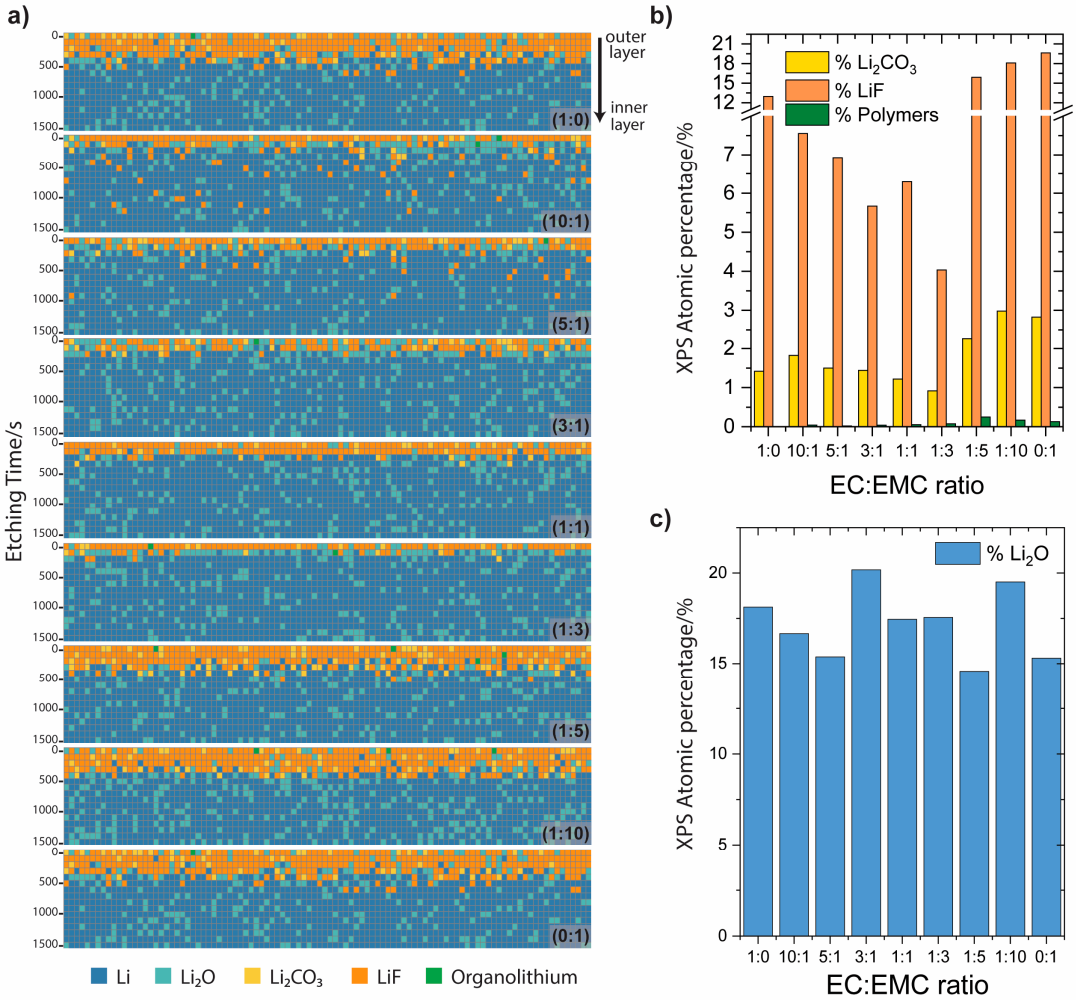

Figure 4. C 1s XPS analysis results for Li metal samples after electrolyte immersion. (**a**) Heatmap-style representation of atomic percentages from C 1s XPS analyses of Li metal immersed in electrolytes with various EC:EMC ratios (1:0, 10:1, 5:1, 3:1, 1:1, 1:3, 1:5, 1:10, and 0:1), each containing 1 M $LiPF_6$, (**b**) total percentages of Li_2CO_3, LiF, and organolithium compounds identified in part (**a**), and (**c**) total percentages of Li_2O detected in the samples.

The results imply that although LiF is essential for stabilizing the SEI, its effectiveness is significantly influenced by the distribution of components and the presence of Li_2CO_3. In the 1:3 EC:EMC sample, the LiF content is moderate while the Li_2CO_3 content is low, potentially leading to a reduced cycle life. This observation suggests that an optimal balance between LiF and Li_2CO_3 is necessary to ensure proper SEI stability and, consequently, a longer cycle life. Samples with higher Li_2CO_3 content (e.g., 1:5, 1:10, 0:1) show increased resilience and longer cycle life. Conversely, samples with higher LiF content and lower

Li_2CO_3 (e.g., 1:0, 10:1, 5:1, 3:1, 1:1) also exhibit reduced cycle life. These findings indicate that both components must be balanced for optimal performance.

Electrolyte solutions with EC:EMC ratios of 10:1, 5:1, 3:1, and 1:1 effectively reduced the side reactions between Li and organic solvents, alleviated rapid cycling drops, and facilitated the formation of a more beneficial mixture of inorganic components in the SEI. The Li_2O content across all the samples remained relatively constant, ranging as 15–20%, indicating that it was not significantly affected by variations in the solvent composition within the electrolyte. Consequently, the reactions involving Li_2O were not considered in this analysis. In general, the sub-products formed at 1:1 and 1:3 ratios, featuring lower total mixed Li_2CO_3 and moderate levels of LiF mixed with organolithium compounds, functioned as better passivating agents than those with a higher content of Li_2CO_3, and higher levels of LiF, ROLi, and $ROCO_2Li$. This balance is due to the moderate levels of these components providing sufficient passivation without making the SEI overly rigid and prone to cracking. This observation is consistent with studies demonstrating that the reduction products of moderate amounts of EC are insoluble, thus providing more effective passivation [19].

4. Discussion

As the analysis progressed, it became crucial to examine the chemical reactions occurring within the electrolyte, particularly those that facilitated the formation of Li_2CO_3. Figure 5 provides a schematic of the reactions and consequent generation of Li_2CO_3, along with other byproducts. The chemical reactions depicted in Figure 5 illustrate that the SEI film exhibited a complex layered structure that was significantly affected by the EC:EMC ratio. This study demonstrated that modifying these ratios influenced the formation of Li_2CO_3, LiF, and organolithium compounds, as evidenced by XPS analysis. These findings indicate that the solvent composition significantly affected the formation of the SEI, which is critical for the cycling performance of Li metal batteries.

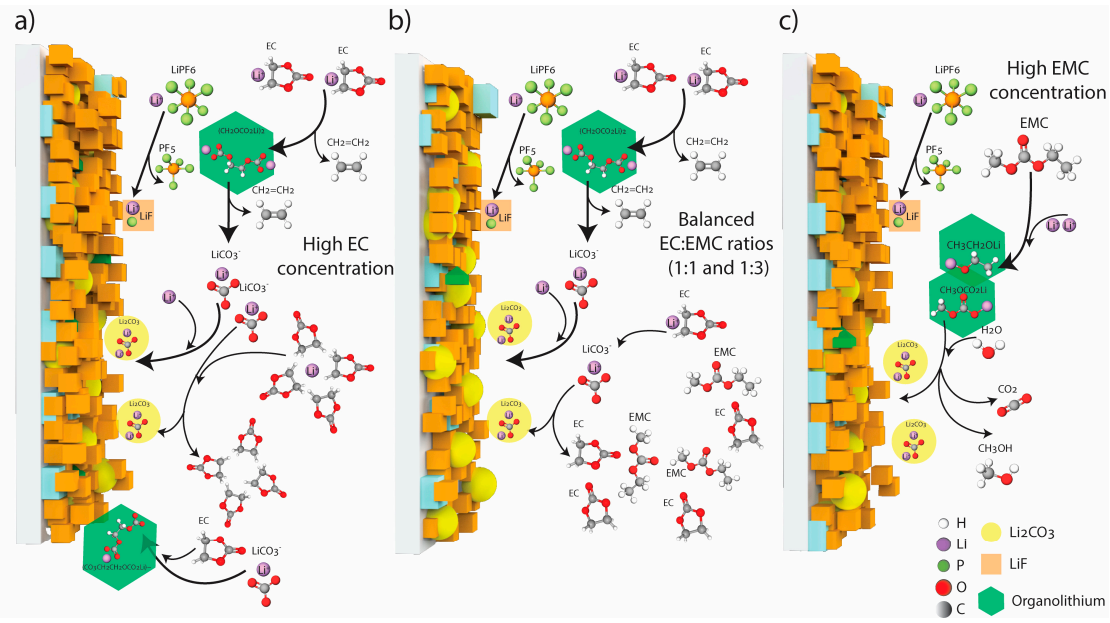

Figure 5. Schematic of the reduction mechanisms of EC and EMC under different conditions: (**a**) high EC concentrations, (**b**) balanced EC:EMC ratios, such as 1:1 and 1:3, and (**c**) high EMC concentrations.

The reduction patterns indicated that Li_2CO_3 was more prevalent at both high and low EC concentrations for several reasons. At high EC concentrations, the reaction pathways directly formed Li_2CO_3 (Figure 5a), whereas at low EC concentrations (high EMC concentration), the presence of water may disrupt reactions, resulting in the formation of Li_2CO_3 (Figure 5c). Studies have demonstrated that the organic components within the

SEI enhance its flexibility and durability, whereas the inorganic species contribute to its rigidity [36,37]. The predominance of inorganic materials, coupled with the low organic content, as observed in electrolyte solutions with ratios of 1:5, 1:10, and 0:1, rendered the surface films highly rigid. This rigidity rendered them susceptible to cracking during the expansion and contraction associated with Li metal deposition and stripping, as shown in Figure 1, leading to shortened cycle life of the samples. Therefore, this type of SEI cannot effectively prevent the continuous reaction between the Li metal and electrolyte, resulting in persistent electrolyte consumption, shortened voltage cycling, and low lithium plating/stripping efficiency, which is consistent with the experimental findings presented in Figure 1. These electrolyte ratios are identified as the worst-performing due to their poor cycle life.

In contrast to the two previous schema systems, the SEI formed at EC:EMC ratios of 1:1 and 1:3 exhibited a balanced intermediate state without significant formation of Li_2CO_3, LiF, or organolithium products (Figure 5b). This observation is not attributable to shorter reaction pathways or limited product formation; rather, it reflects a specific affinity between EC, EMC, and lithium. This affinity indicates the significant contribution of solvent molecules to SEI formation, which inhibits extensive decomposition and results in an optimal SEI layer, as reported by Zhang et al. [38]. Consequently, the decomposition of the lithium salt in the electrolyte solution was suppressed, resulting in minimal LiF and inorganic accumulation within the SEI. This process enhanced the lithium ion diffusion along the SEI and lithium metal interface, driven by the affinity between lithium metal and lithium ions [39], thereby improving cell cycle stability, as shown in Figure 1. The 1:1 ratio is identified as the best-performing electrolyte due to its superior balance and enhanced cycle stability, while the 1:3 ratio is considered a moderate-performing electrolyte because, although it has high ionic conductivity and capacity, it results in a lower cycle life compared to the 1:1 ratio. This phenomenon underscores the significant contribution of both Li_2CO_3 and LiF to the uniformity of the formed SEI. The uniform SEI, characterized by a balanced mix of inorganic and organic species, likely exhibited both rigidity and flexibility. This balance is crucial for stabilizing and protecting Li metal. Although organolithium interactions were limited in the XPS analysis, as observed in the FTIR spectra, the low organolithium content may suggest either a minimal contribution of solvent molecules to SEI formation or high solubility of the formed organic species.

5. Conclusions

This study provides significant insights into the formation of inorganic and organolithium electrolyte derivatives that comprise SEI on Li metal electrodes. The unique observations demonstrated that the EC and EMC ratios substantially affected the characteristics of the SEI layer. The presence of inorganic components, particularly Li_2CO_3 and LiF, facilitated the enhancement of, or reduction in, the cycling stability and mechanical robustness of these cells. This can likely be attributed to their superior Li-ion conductivity and mechanical properties, as evidenced by the changes in the SEI thickness observed in the XPS measurements. These results emphasize the crucial role of the EC:EMC ratio in forming an optimal SEI on the lithium metal surface, leading to superior battery performance. Future investigations should focus on the dynamic interactions among solvent molecules to better understand the formation and behavior of H-H coupling in various configurations, including cyclic–linear, linear–linear, and cyclic–cyclic solvent carbonates, both before and after interactions with Li ions from $LiPF_6$. Such studies are essential for the tailoring of electrolyte compositions to optimize the specific characteristics of energy storage systems, thereby enhancing their efficiency and longevity.

Supplementary Materials: The following Supporting Information can be downloaded from: https://www.mdpi.com/article/10.3390/batteries10060210/s1, Figure S1: XPS spectra of the C1s photoemission lines for EC:EMC ratios of (a) 1:0, (b) 10:1, (c) 5:1, (d) 3:1, (e) 1:1, (f) 1:3, (g) 1:5, (h) 1:10, and (i) 0:1, each with 1 M $LiPF_6$. All spectra were calibrated using the contaminant hydrocarbon at 284.9 eV and background-corrected with a Shirley method.; Figure S2: XPS spectra of the O1s photoemission lines for EC:EMC ratios of (a) 1:0, (b) 10:1, (c) 5:1, (d) 3:1, (e) 1:1, (f) 1:3, (g) 1:5, (h) 1:10, and (i) 0:1, each with 1 M $LiPF_6$. All the spectra were calibrated using contaminant hydrocarbon (284.9 eV) and background-corrected using the Shirley method.

Author Contributions: Conceptualization, P.M.N. and S.-K.J.; methodology, P.M.N. and S.L.; formal analysis, P.M.N. and S.Y.; investigation, P.M.N.; resources, P.M.N. and S.Y.; data curation, P.M.N. and S.L.; writing—original draft preparation, P.M.N.; writing review and editing, P.M.N. and S.-K.J.; supervision, S.-K.J.; project administration, S.-K.J.; funding acquisition, S.-K.J. All authors have read and agreed to the published version of the manuscript.

Funding: This research was supported by the Basic Science Research Program through the National Research Foundation of Korea (NRF), funded by the Ministry of Education (NRF-2021R1I1A3060329). This work was supported by the Korea Institute for Advancement of Technology (KIAT) grant funded by the Korean Government (MOTIE) (1415188261, Automotive Industry Technology Development). This study was supported by the Soonchunhyang University Research Fund.

Data Availability Statement: Data is contained within the article or Supplementary Material.

Conflicts of Interest: The authors declare no conflict of interest.

References

1. Xu, K. Electrolytes and Interphases in Li-Ion Batteries and Beyond. *Chem. Rev.* **2014**, *114*, 11503–11618. [CrossRef] [PubMed]
2. Varzi, A.; Thanner, K.; Scipioni, R.; Di Lecce, D.; Hassoun, J.; Dörfler, S.; Altheus, H.; Kaskel, S.; Prehal, C.; Freunberger, S.A. Current Status and Future Perspectives of Lithium Metal Batteries. *J. Power Sources* **2020**, *480*, 228803. [CrossRef]
3. Shen, X.; Zhang, X.-Q.; Ding, F.; Huang, J.-Q.; Xu, R.; Chen, X.; Yan, C.; Su, F.-Y.; Chen, C.-M.; Liu, X.; et al. Advanced Electrode Materials in Lithium Batteries: Retrospect and Prospect. *Energy Mater. Adv.* **2021**, *2021*, 1205324. [CrossRef]
4. Liu, J.; Zhang, Y.; Zhou, J.; Wang, Z.; Zhu, P.; Cao, Y.; Zheng, Y.; Zhou, X.; Yan, C.; Qian, T. Advances and Prospects in Improving the Utilization Efficiency of Lithium for High Energy Density Lithium Batteries. *Adv. Funct. Mater.* **2023**, *33*, 2302055. [CrossRef]
5. Ding, M.S.; Xu, K.; Zhang, S.; Jow, T.R. Liquid/Solid Phase Diagrams of Binary Carbonates for Lithium Batteries Part II. *J. Electrochem. Soc.* **2001**, *148*, A299–A304. [CrossRef]
6. Aurbach, D.; Levi, M.D.; Levi, E.; Schechter, A. Failure and Stabilization Mechanisms of Graphite Electrodes. *J. Phys. Chem. B* **1997**, *101*, 2195–2206. [CrossRef]
7. Ein-Eli, Y.; McDevitt, S.F.; Laura, R. The Superiority of Asymmetric Alkyl Methyl Carbonates. *J. Electrochem. Soc.* **1998**, *145*, L1–L3. [CrossRef]
8. Peled, E. The Electrochemical Behavior of Alkali and Alkaline Earth Metals in Nonaqueous Battery Systems—The Solid Electrolyte Interphase Model. *J. Electrochem. Soc.* **1979**, *126*, 2047–2051. [CrossRef]
9. Peled, E.; Golodnitsky, D.; Menachem, C.; Bartow, D. An Advanced Tool for the Selection of Electrolyte Components for Rechargeable Lithium Batteries. *J. Electrochem. Soc.* **1998**, *145*, 3482–3486. [CrossRef]
10. Aurbach, D.; Ein-Eli, Y.; Markovsky, B.; Zaban, A.; Luski, S.; Carmeli, Y.; Yamin, H. The Study of Electrolyte Solutions Based on Ethylene and Diethyl Carbonates for Rechargeable Li Batteries: II. Graphite Electrodes. *J. Electrochem. Soc.* **1995**, *142*, 2882–2890. [CrossRef]
11. Zhang, S.; Ding, M.S.; Xu, K.; Allen, J.; Jow, T.R. Understanding Solid Electrolyte Interface Film Formation on Graphite Electrodes. *ECS Electrochem. Lett.* **2001**, *4*, A206–A208. [CrossRef]
12. Fong, R.; von Sacken, U.; Dahn, J.R. Studies of Lithium Intercalation into Carbons Using Nonaqueous Electrochemical Cells. *J. Electrochem. Soc.* **1990**, *137*, 2009–2013. [CrossRef]
13. Guyomard, D.; Tarascon, J.M. Rechargeable $Li_{1+x}Mn_2O_4$/Carbon Cells with a New Electrolyte Composition: Potentiostatic Studies and Application to Practical Cells. *J. Electrochem. Soc.* **1993**, *140*, 3071–3081. [CrossRef]
14. Tarascon, J.; Guyomard, D. New Electrolyte Compositions Stable over the 0 to 5 V Voltage Range and Compatible with the $Li_{1+x}Mn_2O_4$/Carbon Li-Ion Cells. *Solid State Ion.* **1994**, *69*, 293–305. [CrossRef]
15. Wilken, S.; Treskow, M.; Scheers, J.; Johansson, P.; Jacobsson, P. Initial Stages of Thermal Decomposition of $LiPF_6$-Based Lithium Ion Battery Electrolytes by Detailed Raman and NMR Spectroscopy. *RSC Adv.* **2013**, *3*, 16359–16364. [CrossRef]
16. Aurbach, D.; Gofer, Y.; Ben-Zion, M.; Aped, P. The Behaviour of Lithium Electrodes in Propylene and Ethylene Carbonate: Te Major Factors That Influence Li Cycling Efficiency. *J. Electroanal. Chem.* **1992**, *339*, 451–471. [CrossRef]
17. Aurbach, D.; Markovsky, B.; Weissman, I.; Levi, E.; Ein-Eli, Y. On the Correlation between Surface Chemistry and Performance of Graphite Negative Electrodes for Li Ion Batteries. *Electrochim. Acta* **1999**, *45*, 67–86. [CrossRef]

18. Wang, Y.; Nakamura, S.; Ue, M.; Balbuena, P.B. Theoretical Studies to Understand Surface Chemistry on Carbon Anodes for Lithium-Ion Batteries: Reduction Mechanisms of Ethylene Carbonate. *J. Am. Chem. Soc.* **2001**, *123*, 11708–11718. [CrossRef] [PubMed]
19. Aurbach, D.; Markovsky, B.; Shechter, A.; Ein-Eli, Y.; Cohen, H. A Comparative Study of Synthetic Graphite and Li Electrodes in Electrolyte Solutions Based on Ethylene Carbonate-Dimethyl Carbonate Mixtures. *J. Electrochem. Soc.* **1996**, *143*, 3809–3820. [CrossRef]
20. Wang, Y.; Balbuena, P.B. Theoretical Studies on Cosolvation of Li Ion and Solvent Reductive Decomposition in Binary Mixtures of Aliphatic Carbonates. *Int. J. Quantum Chem.* **2005**, *102*, 724–733. [CrossRef]
21. Leung, K. Two-Electron Reduction of Ethylene Carbonate: A Quantum Chemistry Re-Examination of Mechanisms. *Chem. Phys. Lett.* **2013**, *568–569*, 1–8. [CrossRef]
22. Yu, J.; Balbuena, P.B.; Budzien, J.; Leung, K. Hybrid DFT Functional-Based Static and Molecular Dynamics Studies of Excess Electron in Liquid Ethylene Carbonate. *J. Electrochem. Soc.* **2011**, *158*, A400–A410. [CrossRef]
23. Islam, M.M.; Van Duin, A.C.T. Reductive Decomposition Reactions of Ethylene Carbonate by Explicit Electron Transfer from Lithium: An EReaxFF Molecular Dynamics Study. *J. Phys. Chem. C* **2016**, *120*, 27128–27134. [CrossRef]
24. Martinez De La Hoz, J.M.; Leung, K.; Balbuena, P.B. Reduction Mechanisms of Ethylene Carbonate on Si Anodes of Lithium-Ion Batteries: Effects of Degree of Lithiation and Nature of Exposed Surface. *ACS Appl. Mater. Interfaces* **2013**, *5*, 13457–13465. [CrossRef] [PubMed]
25. Leung, K.; Budzien, J.L. Ab Initio Molecular Dynamics Simulations of the Initial Stages of Solid-Electrolyte Interphase Formation on Lithium Ion Battery Graphitic Anodes. *Phys. Chem. Chem. Phys.* **2010**, *12*, 6583–6586. [CrossRef] [PubMed]
26. Kominato, A.; Yasukawa, E.; Sato, N.; Ijuuin, T.; Asahina, H.; Mori, S. Analysis of surface films on lithium in various organic electrolytes. *J. Power Sources* **1997**, *68*, 471–475. [CrossRef]
27. Matsuda, Y.; Morita, M.; Yamada, K.; Hirai, K. Characteristics of Sulfolane-Based Electrolytes for Rechargeable Lithium Batteries. *J. Electrochem. Soc.* **1985**, *132*, 2538–2543. [CrossRef]
28. Fan, H.; Gao, J.; Qi, L.; Wang, H. Hexafluorophosphate Anion Intercalation into Graphite Electrode from Sulfolane/Ethylmethyl Carbonate Solutions. *Electrochim. Acta* **2016**, *189*, 9–15. [CrossRef]
29. Xu, K. Nonaqueous Liquid Electrolytes for Lithium-Based Rechargeable Batteries. *Chem. Rev.* **2004**, *104*, 4303–4417. [CrossRef] [PubMed]
30. Borodin, O.; Smith, G.D. Quantum Chemistry and Molecular Dynamics Simulation Study of Dimethyl Carbonate: Ethylene Carbonate Electrolytes Doped with LiPF6. *J. Phys. Chem. B* **2009**, *113*, 1763–1776. [CrossRef] [PubMed]
31. Zhang, S.S. A Review on Electrolyte Additives for Lithium-Ion Batteries. *J. Power Sources* **2006**, *162*, 1379–1394. [CrossRef]
32. Fu, A.; Lin, J.; Zhang, Z.; Xu, C.; Zou, Y.; Liu, C.; Yan, P.; Wu, D.Y.; Yang, Y.; Zheng, J. Synergistical Stabilization of Li Metal Anodes and $LiCoO_2$ Cathodes in High-Voltage Li||$LiCoO_2$ Batteries by Potassium Selenocyanate (KSeCN) Additive. *ACS Energy. Lett.* **2022**, *7*, 1364–1373. [CrossRef]
33. He, M.; Guo, R.; Hobold, G.M.; Gao, H.; Gallant, B.M. The Intrinsic Behavior of Lithium Fluoride in Solid Electrolyte Interphases on Lithium. *Proc. Natl. Acad. Sci. USA* **2020**, *117*, 73–79. [CrossRef] [PubMed]
34. Tan, Y.H.; Lu, G.X.; Zheng, J.H.; Zhou, F.; Chen, M.; Ma, T.; Lu, L.L.; Song, Y.H.; Guan, Y.; Wang, J.; et al. Lithium Fluoride in Electrolyte for Stable and Safe Lithium-Metal Batteries. *Adv. Mater.* **2021**, *33*, 2102134. [CrossRef]
35. Li, G.; Duan, X.; Liu, X.; Zhan, R.; Wang, X.; Du, J.; Chen, Z.; Li, Y.; Cai, Z.; Shen, Y.; et al. Locking Active Li Metal through Localized Redistribution of Fluoride Enabling Stable Li-Metal Batteries. *Adv. Mater.* **2023**, *35*, 2207310. [CrossRef]
36. Tong, B.; Huang, J.; Zhou, Z.; Peng, Z. The Salt Matters: Enhanced Reversibility of Li–O_2 Batteries with a Li[(CF_3SO_2)(n-$C_4F_9SO_2$)N]-Based Electrolyte. *Adv. Mater.* **2018**, *30*, 1704841. [CrossRef]
37. Gu, Y.; Wang, W.W.; Li, Y.J.; Wu, Q.H.; Tang, S.; Yan, J.W.; Zheng, M.S.; Wu, D.Y.; Fan, C.H.; Hu, W.Q.; et al. Designable Ultra-Smooth Ultra-Thin Solid-Electrolyte Interphases of Three Alkali Metal Anodes. *Nat. Commun.* **2018**, *9*, 1339. [CrossRef] [PubMed]
38. Zhang, X.; Xu, P.; Duan, J.; Lin, X.; Sun, J.; Shi, W.; Xu, H.; Dou, W.; Zheng, Q.; Yuan, R.; et al. A Dicarbonate Solvent Electrolyte for High Performance 5 V-Class Lithium-Based Batteries. *Nat. Commun.* **2024**, *15*, 536. [CrossRef] [PubMed]
39. Liu, S.; Ji, X.; Yue, J.; Hou, S.; Wang, P.; Cui, C.; Chen, J.; Shao, B.; Li, J.; Han, F.; et al. High Interfacial-Energy Interphase Promoting Safe Lithium Metal Batteries. *J. Am. Chem. Soc.* **2020**, *142*, 2438–2447. [CrossRef]